THE ASTRONOMICAL JOURNAL, 115:2515–2526, 1998 June

CS 22966−043: A BRIGHT NEW FIELD SX PHOENICIS STAR SIMILAR TO THOSE IN NGC 5053

GEORGE W. PRESTON
Carnegie Observatories, Carnegie Institution of Washington, 813 Santa Barbara Street, Pasadena, CA 91101; gwp@ociw.edu

AND

ARLO U. LANDOLT
Department of Physics and Astronomy, Louisiana State University, Baton Rouge, LA 70803-4001; landolt@rouge.phys.lsu.edu
Received 1997 December 29; revised 1998 February 9

ABSTRACT

CS 22966−043 is an ultra–short-period pulsating star with high velocity (RV = −266 km s^{-1}) discovered during the course of a search for spectroscopic binaries among blue metal-poor field stars, in progress since 1992. With respect to period (0.0374 days), mean color ($\langle B-V \rangle = 0.24$), and metal abundance ([Fe/H] ≈ −2.4), it closely resembles the SX Phoenicis stars found among the blue stragglers in NGC 5053. CS 22966−043 also is the primary of a spectroscopic binary with (probable) period of 430 days. Light-travel time across the projected orbit, as large as 0.0037 days, must be added to the times of observation to combine data obtained in different years with minimal phase dispersion. If CS 22966−043 is, indeed, a blue straggler formed by binary interaction as is now generally believed, then it seems most probable that the interaction was one of mass transfer from the present-day secondary during its post–main-sequence evolution rather than merger of a close binary. The latter option would require that this rare field star was, in addition, a member of a primordial triple system.

Key words: binaries: spectroscopic — stars: variables: other

1. INTRODUCTION

CS 22966−043 is one of 62 blue metal-poor (BMP) stars monitored for radial velocity variations since 1992 (Preston 1995). It has been argued elsewhere (Preston, Beers, & Shectman 1994) that the BMP sample probably contains a mixture of globular cluster–like blue stragglers and intermediate-age main-sequence stars accreted from satellites of the Milky Way. The purpose of the radial velocity survey is to determine the spectroscopic binary fraction of this mixture. Typically, two or more echelle spectra (resolution ∼25,000) of each star in the program have been obtained annually. Numerous binaries have been discovered and orbital elements derived. However, CS 22966−043 remained intractable through 1995. In spite of a sizable velocity range (∼30 km s^{-1}), no period in the interval 1–1000 days could be found. Accordingly, tactics were changed in 1996. Series of 10 minute echelle exposures by G. W. P. in 1996 August showed immediately that the velocity varied on a timescale of 1 hr. A. U. L. undertook *UBV* photometric observations shortly thereafter. More spectroscopic and photometric observations were obtained in 1997, and we summarize the results of these efforts here.

2. OBSERVATIONS

2.1. *Spectroscopy*

Sixty spectroscopic observations of CS 22966−043 were obtained in the years 1992 through 1997 with the echelle spectrograph of the Las Campanas 2.5 m telescope. The "2D-FRUTTI" spectra (Shectman 1984) were sky-subtracted, divided by nightly flat-field images, and rectified. The extracted spectra were then corrected for scattered light and were wavelength-calibrated by hollow-cathode thorium-argon spectra recorded immediately after each single stellar observation in 1992–1995, and before and after each series of spectra in 1996 and 1997. All these reductions were accomplished with a suite of software written by S. Shectman and J. Bechtold. Radial velocities were obtained by cross-correlation of each stellar spectrum with a standard-star template as described in Preston (1994). A standard system of radial velocities is defined by numerous observations of constant BMP stars in each observing run. Typical rms scatter of constant stars with spectra similar to that of CS 22966−043 is less than 1 km s^{-1}. No secular drift of the velocity system defined by BMP standard stars as large as 1 km s^{-1} has been detected from 1992 through 1997.

The spectroscopic observations are listed in Table 1, which contains in successive columns the echelle frame number, Heliocentric Julian Date of the midpoint of the observation, Heliocentric Julian Date corrected for orbital light-travel time (see § 4), pulsation phase, observed radial velocity of each spectrum, and radial velocity shifted to the 1996 pulsation curve by adding the correction $\langle \mathrm{RV(1996)} \rangle - \langle \mathrm{RV(yr)} \rangle$ formed from data in Table 3 below.

2.2. *Photometry*

The photometric observations were obtained by A. U. L. at the Yale 1.0 m and 1.5 m telescopes of the Cerro Tololo Inter-American Observatory (CTIO). A. U. L.'s C31034A GaAs photomultiplier, CTIO's *UBVRI* filter set No. 3, and CTIO's standard photoelectric data acquisition system, the same combination used for his standard-star work, were used to obtain observations through the *UBV* filters on nine nights in 1996 and three nights in 1997. Data were obtained in a series of measurements *VBUUBV*, each measurement normally of 10 s duration per filter. Extinction corrections and nonlinear transformations from instrumental to standard magnitudes and color indexes were performed for the reasons and according to the procedures described by Landolt (1992). These efforts, together with the equipment utilized, ensured that the final reduced data were on the photometric system defined by that paper.

TABLE 1

Spectroscopic Observations of CS 22966−043

Frame	HJD (2,400,000+)	HJD + t_{orb}	$n + \varphi$	RV_{obs} (km s^{-1})	RV_{corr} (km s^{-1})
92173......	48,813.8269	48,813.8269	0.546	−273.5	−268.2
92230......	48,823.7496	48,823.7496	265.685	−269.1	−263.8
93188......	49,194.7680	49,194.7688	10179.491	−280.4	−268.1
93395......	49,207.7626	49,207.7631	10526.706	−280.1	−267.8
94113......	49,573.7997	49,573.8018	20307.431	−287.2	−274.9
94352......	49,579.8119	49,579.8139	20468.078	−260.9	−248.6
94508......	49,584.7270	49,584.7289	20599.410	−288.4	−276.1
94555......	49,588.7661	49,588.7679	20707.334	−283.6	−271.3
94594......	49,590.7602	49,590.7619	20760.613	−285.6	−273.3
94651......	49,592.6852	49,592.6869	20812.051	−261.3	−249.0
95121......	49,933.8284	49,933.8320	29927.609	−282.3	−274.0
95261......	49,936.7336	49,936.7371	30005.234	−268.1	−259.8
95325......	49,937.8076	49,937.8111	30033.932	−256.9	−248.6
95390......	49,939.7087	49,939.7122	30084.730	−270.2	−261.9
95485......	49,944.7809	49,944.7843	30220.259	−271.0	−262.7
95535......	49,945.8209	49,945.8243	30248.049	−255.5	−247.2
96233......	50,289.7309	50,289.7342	39437.484	−275.4	−275.4
96234......	50,289.7419	50,289.7452	39437.778	−258.1	−258.1
96235......	50,289.7519	50,289.7552	39438.045	−247.6	−247.6
96236......	50,289.7629	50,289.7662	39438.339	−269.9	−269.9
96238......	50,289.7769	50,289.7802	39438.713	−262.4	−262.4
96239......	50,289.7859	50,289.7892	39438.954	−246.5	−246.5
96240......	50,289.7929	50,289.7962	39439.141	−252.1	−252.1
96241......	50,289.8009	50,289.8042	39439.355	−274.1	−274.1
96242......	50,289.8069	50,289.8102	39439.515	−276.2	−276.2
96243......	50,289.8139	50,289.8172	39439.702	−262.7	−262.7
96365......	50,291.7280	50,291.7313	39490.848	−254.4	−254.4
96366......	50,291.7350	50,291.7383	39491.035	−245.7	−245.7
96367......	50,291.7420	50,291.7453	39491.222	−260.1	−260.1
96368......	50,291.7490	50,291.7523	39491.409	−275.9	−275.9
96369......	50,291.7560	50,291.7593	39491.596	−272.9	−272.9
96370......	50,291.7630	50,291.7663	39491.783	−257.4	−257.4
96372......	50,291.7740	50,291.7773	39492.077	−249.2	−249.2
96373......	50,291.7810	50,291.7843	39492.264	−268.2	−268.2
96374......	50,291.7880	50,291.7913	39492.451	−278.9	−278.9
96375......	50,291.7950	50,291.7983	39492.638	−269.0	−269.0
96376......	50,291.8020	50,291.8053	39492.825	−253.2	−253.2
96377......	50,291.8090	50,291.8123	39493.012	−246.6	−246.6
96378......	50,291.8170	50,291.8203	39493.226	−260.7	−260.7
96427......	50,292.7071	50,292.7105	39517.011	−246.1	−246.1
96428......	50,292.7141	50,292.7175	39517.198	−258.9	−258.9
96429......	50,292.7211	50,292.7245	39517.385	−276.4	−276.4
96430......	50,292.7281	50,292.7315	39517.572	−273.1	−273.1
96431......	50,292.7351	50,292.7385	39517.760	−258.4	−258.4
96433......	50,292.7461	50,292.7495	39518.053	−248.0	−248.0
96434......	50,292.7531	50,292.7565	39518.241	−263.5	−263.5
97325......	50,646.7864	50,646.7882	48978.134	−251.8	−255.0
97326......	50,646.7934	50,646.7952	48978.321	−272.8	−276.0
97327......	50,646.8004	50,646.8022	48978.508	−271.0	−274.2
97328......	50,646.8084	50,646.8102	48978.722	−254.8	−258.0
97329......	50,646.8154	50,646.8172	48978.909	−245.6	−248.8
97330......	50,646.8224	50,646.8242	48979.096	−246.9	−250.1
97331......	50,646.8294	50,646.8312	48979.283	−267.9	−271.1
97662......	50,704.6830	50,704.6861	50525.194	−253.6	−253.3
97664......	50,704.6941	50,704.6972	50525.491	−279.7	−279.4
97665......	50,704.7011	50,704.7042	50525.676	−268.3	−268.0
97666......	50,704.7080	50,704.7111	50525.862	−252.8	−252.5
97667......	50,704.7150	50,704.7181	50526.048	−245.5	−245.2
97668......	50,704.7226	50,704.7257	50526.252	−261.0	−260.7
97670......	50,704.7351	50,704.7382	50526.586	−275.6	−275.3

The photometric observations are listed in Table 2, which contains in successive columns the Heliocentric Julian Date for the midpoint of each complete measurement (i.e., the midpoint of each *VBUUBV* data set), the Heliocentric Julian Date corrected for orbital light-travel time, pulsation phase calculated from equation (1) in § 2 below, and then the V, $B-V$, and $U-B$ magnitude and color indexes.

3. PULSATION CYCLE

3.1. *Radial Velocity Variation*

A period of approximately 0.0374 days was derived immediately from the 1996 spectroscopic and photometric data, but the period is so short that the cycle count was uncertain between the spectroscopic and photometric

TABLE 2

PHOTOMETRIC OBSERVATIONS OF CS 22966−043

HJD (2,400,000 +)	HJD + t_{orb}	$n + \varphi$	V	$B-V$	$U-B$
50,312.8597......	50,312.8633	40,055.504	13.493	0.229	−0.018
50,312.8658......	50,312.8694	40,055.667	13.540	0.253	−0.040
50,312.8719......	50,312.8755	40,055.830	13.564	0.253	−0.034
50,312.8780......	50,312.8816	40,055.993	13.553	0.233	−0.044
50,312.8840......	50,312.8876	40,056.152	13.505	0.246	−0.062
50,312.8898......	50,312.8934	40,056.309	13.452	0.216	−0.025
50,312.8957......	50,312.8993	40,056.466	13.471	0.225	−0.026
50,312.9015......	50,312.9051	40,056.622	13.531	0.233	0.017
50,312.9074......	50,312.9110	40,056.777	13.551	0.271	−0.064
50,314.8427......	50,314.8463	40,108.489	13.477	0.223	−0.030
50,314.8489......	50,314.8525	40,108.655	13.520	0.249	−0.040
50,314.8549......	50,314.8585	40,108.816	13.543	0.262	−0.049
50,314.8609......	50,314.8645	40,108.977	13.553	0.251	−0.071
50,314.8669......	50,314.8705	40,109.136	13.526	0.237	−0.059
50,314.8728......	50,314.8764	40,109.295	13.444	0.245	−0.055
50,314.8788......	50,314.8824	40,109.455	13.472	0.217	−0.036
50,314.8848......	50,314.8884	40,109.617	13.515	0.261	−0.059
50,314.8909......	50,314.8944	40,109.775	13.555	0.259	−0.065
50,314.8967......	50,314.9003	40,109.933	13.564	0.247	−0.063
50,314.9025......	50,314.9061	40,110.089	13.542	0.258	−0.075
50,314.9088......	50,314.9124	40,110.256	13.465	0.231	−0.066
50,315.8224......	50,315.8260	40,134.669	13.536	0.230	−0.047
50,315.8250......	50,315.8286	40,134.739	13.532	0.279	−0.076
50,315.8282......	50,315.8318	40,134.824	13.570	0.248	−0.075
50,315.8319......	50,315.8355	40,134.922	13.565	0.257	−0.064
50,315.8346......	50,315.8382	40,134.993	13.563	0.260	−0.091
50,315.8374......	50,315.8410	40,135.069	13.560	0.255	−0.055
50,315.8405......	50,315.8441	40,135.151	13.538	0.224	−0.047
50,315.8431......	50,315.8467	40,135.222	13.503	0.250	−0.076
50,315.8457......	50,315.8493	40,135.292	13.475	0.225	−0.050
50,315.8484......	50,315.8520	40,135.362	13.469	0.238	−0.048
50,315.8510......	50,315.8546	40,135.433	13.481	0.237	−0.079
50,315.8537......	50,315.8573	40,135.505	13.518	0.211	−0.032
50,315.8563......	50,315.8599	40,135.575	13.539	0.232	−0.059
50,315.8591......	50,315.8627	40,135.648	13.553	0.248	−0.033
50,315.8618......	50,315.8654	40,135.720	13.564	0.269	−0.054
50,315.8644......	50,315.8680	40,135.791	13.586	0.262	−0.066
50,315.8671......	50,315.8707	40,135.863	13.587	0.258	−0.070
50,315.8698......	50,315.8734	40,135.935	13.576	0.257	−0.059
50,315.8725......	50,315.8761	40,136.007	13.561	0.262	−0.070
50,315.8751......	50,315.8787	40,136.078	13.566	0.253	−0.073
50,315.8780......	50,315.8816	40,136.155	13.526	0.242	−0.062
50,315.8805......	50,315.8841	40,136.220	13.489	0.249	...
50,315.8829......	50,315.8865	40,136.284	13.446	0.225	−0.020
50,315.8855......	50,315.8891	40,136.354	13.437	0.214	−0.054
50,315.8882......	50,315.8918	40,136.426	13.445	0.258	−0.053
50,315.8908......	50,315.8944	40,136.497	13.475	0.237	−0.048
50,315.8935......	50,315.8971	40,136.568	13.499	0.244	−0.024
50,315.8962......	50,315.8998	40,136.640	13.525	0.263	−0.070
50,315.8988......	50,315.9024	40,136.710	13.547	0.259	−0.072
50,316.7226......	50,316.7262	40,158.722	13.543	0.267	−0.059
50,316.7252......	50,316.7288	40,158.791	13.563	0.263	−0.062
50,316.7304......	50,316.7340	40,158.931	13.431	0.306	−0.136
50,316.7326......	50,316.7362	40,158.989	13.558	0.254	−0.050
50,316.7352......	50,316.7388	40,159.058	13.559	0.234	−0.040
50,316.7379......	50,316.7415	40,159.131	13.539	0.237	−0.064
50,316.7405......	50,316.7441	40,159.200	13.497	0.243	−0.084
50,316.7431......	50,316.7467	40,159.270	13.466	0.208	−0.026
50,316.7457......	50,316.7493	40,159.339	13.451	0.238	−0.071
50,316.7483......	50,316.7519	40,159.409	13.465	0.222	−0.050
50,316.7510......	50,316.7546	40,159.480	13.484	0.231	−0.030
50,316.7537......	50,316.7573	40,159.553	13.520	0.227	−0.044
50,316.7563......	50,316.7599	40,159.623	13.541	0.243	−0.036
50,316.7591......	50,316.7627	40,159.698	13.564	0.256	−0.077
50,316.7617......	50,316.7653	40,159.768	13.575	0.264	−0.089
50,316.7644......	50,316.7680	40,159.841	13.577	0.244	−0.059
50,316.7673......	50,316.7709	40,159.916	13.583	0.254	−0.070
50,316.7699......	50,316.7735	40,159.985	13.569	0.248	−0.060
50,316.7725......	50,316.7761	40,160.057	13.560	0.246	−0.086
50,316.7753......	50,316.7789	40,160.129	13.533	0.240	−0.064
50,316.7779......	50,316.7815	40,160.199	13.499	0.240	−0.046
50,316.7805......	50,316.7841	40,160.269	13.475	0.213	−0.051

TABLE 2—*Continued*

HJD (2,400,000 +)	HJD + t_{orb}	$n + \varphi$	V	$B-V$	$U-B$
50,316.7831......	50,316.7867	40,160.338	13.449	0.208	−0.017
50,316.7857......	50,316.7893	40,160.408	13.480	0.179	0.000
50,316.7883......	50,316.7919	40,160.479	13.495	0.226	−0.059
50,316.7911......	50,316.7947	40,160.551	13.514	0.248	−0.044
50,316.7937......	50,316.7973	40,160.622	13.548	0.223	−0.040
50,316.7963......	50,316.7999	40,160.692	13.553	0.269	−0.087
50,316.7989......	50,316.8025	40,160.762	13.567	0.250	−0.064
50,316.8015......	50,316.8051	40,160.832	13.589	0.237	−0.057
50,316.8042......	50,316.8078	40,160.903	13.572	0.259	−0.070
50,316.8070......	50,316.8106	40,160.976	13.578	0.257	−0.065
50,316.8096......	50,316.8132	40,161.047	13.563	0.252	−0.081
50,316.8122......	50,316.8158	40,161.118	13.543	0.244	−0.056
50,316.8148......	50,316.8184	40,161.187	13.502	0.249	−0.051
50,316.8175......	50,316.8211	40,161.257	13.482	0.232	−0.077
50,316.8200......	50,316.8236	40,161.326	13.468	0.228	−0.063
50,316.8227......	50,316.8263	40,161.397	13.474	0.207	−0.038
50,316.8253......	50,316.8289	40,161.465	13.487	0.213	−0.033
50,316.8280......	50,316.8316	40,161.537	13.510	0.238	−0.045
50,316.8307......	50,316.8343	40,161.610	13.532	0.235	−0.045
50,316.8333......	50,316.8369	40,161.680	13.542	0.245	−0.041
50,316.8359......	50,316.8395	40,161.749	13.569	0.247	−0.068
50,316.8386......	50,316.8422	40,161.821	13.591	0.245	−0.070
50,316.8419......	50,316.8455	40,161.909	13.571	0.255	−0.051
50,316.8445......	50,316.8481	40,161.979	13.569	0.246	−0.066
50,316.8472......	50,316.8508	40,162.051	13.569	0.228	−0.061
50,318.7338......	50,318.7375	40,212.465	13.460	0.221	−0.057
50,318.7364......	50,318.7401	40,212.536	13.485	0.252	−0.054
50,318.7396......	50,318.7433	40,212.619	13.490	0.295	−0.063
50,318.7423......	50,318.7460	40,212.691	13.532	0.253	−0.075
50,318.7451......	50,318.7488	40,212.767	13.552	0.256	−0.082
50,318.7478......	50,318.7515	40,212.840	13.542	0.246	−0.046
50,318.7505......	50,318.7541	40,212.910	13.550	0.239	−0.031
50,318.7532......	50,318.7569	40,212.983	13.536	0.249	−0.051
50,318.7558......	50,318.7595	40,213.053	13.540	0.268	−0.085
50,318.7585......	50,318.7622	40,213.124	13.522	0.243	−0.056
50,318.7611......	50,318.7648	40,213.196	13.505	0.236	−0.068
50,318.7638......	50,318.7675	40,213.265	13.441	0.256	−0.040
50,318.7665......	50,318.7702	40,213.338	13.438	0.241	−0.053
50,318.7691......	50,318.7728	40,213.408	13.440	0.234	−0.032
50,318.7718......	50,318.7755	40,213.481	13.469	0.219	−0.023
50,318.7744......	50,318.7781	40,213.550	13.486	0.251	−0.034
50,318.7771......	50,318.7808	40,213.622	13.511	0.245	−0.018
50,318.7797......	50,318.7834	40,213.692	13.547	0.270	−0.066
50,318.7824......	50,318.7861	40,213.763	13.544	0.262	−0.043
50,318.7851......	50,318.7888	40,213.836	13.566	0.274	−0.091
50,318.7877......	50,318.7914	40,213.905	13.571	0.253	−0.048
50,318.7904......	50,318.7941	40,213.978	13.564	0.254	−0.077
50,318.7931......	50,318.7968	40,214.049	13.552	0.239	−0.052
50,318.7964......	50,318.8001	40,214.137	13.538	0.234	−0.041
50,318.7990......	50,318.8027	40,214.207	13.499	0.244	−0.059
50,318.8017......	50,318.8054	40,214.279	13.457	0.244	−0.054
50,318.8043......	50,318.8080	40,214.350	13.444	0.258	−0.080
50,318.8070......	50,318.8107	40,214.421	13.447	0.236	−0.015
50,318.8097......	50,318.8134	40,214.493	13.463	0.239	−0.055
50,318.8123......	50,318.8160	40,214.564	13.503	0.240	−0.027
50,318.8151......	50,318.8188	40,214.636	13.531	0.254	−0.059
50,318.8208......	50,318.8245	40,214.789	13.548	0.276	−0.054
50,318.8287......	50,318.8324	40,215.000	13.550	0.274	−0.074
50,318.8340......	50,318.8377	40,215.141	13.532	0.237	−0.045
50,318.8395......	50,318.8432	40,215.289	13.478	0.242	−0.069
50,318.8422......	50,318.8459	40,215.361	13.443	0.245	−0.032
50,318.8448......	50,318.8485	40,215.431	13.463	0.239	−0.049
50,318.8474......	50,318.8511	40,215.501	13.471	0.243	−0.024
50,318.8501......	50,318.8538	40,215.574	13.494	0.266	−0.041
50,318.8530......	50,318.8567	40,215.650	13.533	0.244	−0.025
50,318.8559......	50,318.8596	40,215.729	13.554	0.277	−0.090
50,318.8588......	50,318.8625	40,215.805	13.572	0.257	−0.071
50,318.8615......	50,318.8652	40,215.877	13.585	0.248	−0.053
50,318.8643......	50,318.8680	40,215.952	13.555	0.259	−0.057
50,318.8696......	50,318.8733	40,216.094	13.540	0.229	−0.042
50,318.8760......	50,318.8797	40,216.264	13.460	0.250	−0.019
50,318.8788......	50,318.8825	40,216.340	13.452	0.231	−0.044
50,318.8816......	50,318.8853	40,216.413	13.459	0.229	−0.023
50,318.8845......	50,318.8882	40,216.491	13.496	0.236	−0.018

TABLE 2—*Continued*

HJD (2,400,000 +)	HJD + t_{orb}	$n + \varphi$	V	$B-V$	$U-B$
50,318.8871......	50,318.8908	40,216.561	13.500	0.275	−0.061
50,318.8898......	50,318.8935	40,216.632	13.514	0.294	−0.067
50,318.8927......	50,318.8964	40,216.710	13.547	0.262	−0.058
50,318.8954......	50,318.8991	40,216.784	13.562	0.283	−0.041
50,318.8992......	50,318.9029	40,216.884	13.587	0.253	−0.051
50,318.9021......	50,318.9058	40,216.962	13.560	0.276	−0.096
50,318.9048......	50,318.9085	40,217.035	13.558	0.238	−0.032
50,318.9075......	50,318.9112	40,217.106	13.535	0.254	−0.046
50,318.9103......	50,318.9140	40,217.181	13.520	0.263	−0.068
50,318.9131......	50,318.9168	40,217.255	13.478	0.241	−0.047
50,318.9159......	50,318.9196	40,217.330	13.459	0.236	−0.046
50,318.9185......	50,318.9222	40,217.400	13.472	0.272	−0.037
50,318.9212......	50,318.9249	40,217.472	13.527	0.264	−0.018
50,318.9238......	50,318.9275	40,217.543	13.548	0.329	−0.047
50,396.5597......	50,396.5627	42,291.990	13.529	0.254	−0.069
50,396.5656......	50,396.5686	42,292.149	13.526	0.208	0.003
50,396.5716......	50,396.5746	42,292.308	13.451	0.229	−0.057
50,396.5742......	50,396.5772	42,292.378	13.439	0.222	−0.031
50,396.5767......	50,396.5797	42,292.447	13.431	0.220	−0.020
50,396.5794......	50,396.5824	42,292.516	13.436	0.237	−0.033
50,396.5819......	50,396.5849	42,292.585	13.477	0.226	−0.038
50,396.5845......	50,396.5875	42,292.654	13.519	0.248	−0.079
50,396.5871......	50,396.5901	42,292.724	13.537	0.248	−0.082
50,396.5898......	50,396.5928	42,292.794	13.539	0.269	−0.090
50,396.5948......	50,396.5978	42,292.929	13.527	0.284	−0.083
50,396.5974......	50,396.6004	42,292.997	13.550	0.245	−0.063
50,396.6000......	50,396.6030	42,293.067	13.542	0.238	−0.084
50,396.6026......	50,396.6056	42,293.138	13.547	0.212	−0.050
50,396.6053......	50,396.6083	42,293.209	13.523	0.225	−0.046
50,396.6079......	50,396.6109	42,293.279	13.516	0.229	−0.062
50,396.6105......	50,396.6135	42,293.350	13.464	0.239	−0.048
50,396.6131......	50,396.6161	42,293.419	13.469	0.219	−0.050
50,396.6158......	50,396.6188	42,293.490	13.460	0.221	−0.009
50,396.6183......	50,396.6213	42,293.558	13.502	0.238	−0.032
50,396.6211......	50,396.6241	42,293.632	13.534	0.236	−0.075
50,396.6238......	50,396.6268	42,293.703	13.550	0.272	−0.090
50,396.6279......	50,396.6309	42,293.813	13.567	0.245	−0.050
50,396.6306......	50,396.6336	42,293.886	13.569	0.271	−0.094
50,397.6025......	50,397.6055	42,319.854	13.561	0.254	−0.080
50,397.6052......	50,397.6082	42,319.926	13.556	0.308	−0.124
50,397.6102......	50,397.6132	42,320.060	13.570	0.239	−0.073
50,397.6129......	50,397.6159	42,320.134	13.533	0.242	−0.104
50,397.6185......	50,397.6215	42,320.282	13.486	0.225	−0.064
50,397.6210......	50,397.6240	42,320.351	13.451	0.230	−0.065
50,397.6237......	50,397.6267	42,320.421	13.462	0.213	−0.042
50,397.6263......	50,397.6293	42,320.492	13.461	0.256	−0.076
50,397.6289......	50,397.6319	42,320.561	13.466	0.272	−0.070
50,397.6317......	50,397.6347	42,320.635	13.503	0.243	−0.065
50,397.6343......	50,397.6373	42,320.704	13.515	0.252	−0.057
50,397.6370......	50,397.6400	42,320.777	13.532	0.266	−0.065
50,397.6421......	50,397.6451	42,320.913	13.574	0.261	−0.113
50,397.6447......	50,397.6477	42,320.984	13.569	0.258	−0.122
50,397.6475......	50,397.6505	42,321.057	13.537	0.277	−0.094
50,397.6502......	50,397.6532	42,321.129	13.540	0.230	−0.062
50,397.6876......	50,397.6906	42,322.129	13.562	0.253	−0.110
50,397.6902......	50,397.6932	42,322.199	13.525	0.218	−0.074
50,397.6929......	50,397.6959	42,322.271	13.473	0.226	−0.072
50,397.6956......	50,397.6986	42,322.342	13.445	0.212	−0.065
50,397.6983......	50,397.7013	42,322.416	13.410	0.267	−0.071
50,397.7010......	50,397.7040	42,322.487	13.439	0.233	−0.060
50,397.7037......	50,397.7067	42,322.559	13.494	0.193	−0.042
50,397.7064......	50,397.7094	42,322.631	13.487	0.258	−0.068
50,397.7091......	50,397.7121	42,322.704	13.524	0.250	−0.063
50,397.7118......	50,397.7148	42,322.776	13.563	0.238	−0.108
50,397.7145......	50,397.7175	42,322.847	13.558	0.243	−0.063
50,397.7171......	50,397.7201	42,322.918	13.558	0.207	−0.099
50,397.7197......	50,397.7227	42,322.987	13.568	0.232	−0.102
50,397.7225......	50,397.7255	42,323.061	13.540	0.261	−0.096
50,397.7252......	50,397.7282	42,323.135	13.504	0.274	−0.108
50,397.7279......	50,397.7309	42,323.205	13.521	0.218	−0.070
50,397.7307......	50,397.7337	42,323.280	13.491	0.197	−0.084
50,397.7333......	50,397.7363	42,323.349	13.441	0.222	−0.080
50,401.5921......	50,401.5951	42,426.459	13.473	0.199	−0.048
50,401.5947......	50,401.5977	42,426.528	13.467	0.236	−0.036

TABLE 2—*Continued*

HJD (2,400,000 +)	HJD + t_{orb}	$n + \varphi$	V	$B-V$	$U-B$
50,401.5972......	50,401.6002	42,426.597	13.507	0.224	−0.046
50,401.5998......	50,401.6028	42,426.665	13.534	0.229	−0.051
50,401.6024......	50,401.6054	42,426.734	13.556	0.216	−0.003
50,401.6051......	50,401.6081	42,426.808	13.554	0.244	−0.031
50,401.6077......	50,401.6107	42,426.877	13.566	0.260	−0.053
50,401.6103......	50,401.6133	42,426.946	13.559	0.277	−0.076
50,401.6154......	50,401.6184	42,427.082	13.558	0.250	−0.074
50,401.6207......	50,401.6237	42,427.223	13.519	0.240	−0.067
50,401.6233......	50,401.6263	42,427.293	13.471	0.236	−0.046
50,401.6263......	50,401.6293	42,427.373	13.469	0.212	−0.054
50,401.6290......	50,401.6320	42,427.444	13.454	0.225	−0.048
50,401.6317......	50,401.6347	42,427.516	13.489	0.218	−0.036
50,401.6343......	50,401.6373	42,427.587	13.495	0.230	−0.036
50,401.6370......	50,401.6400	42,427.659	13.527	0.228	−0.024
50,401.6396......	50,401.6426	42,427.728	13.540	0.258	−0.060
50,401.6422......	50,401.6452	42,427.797	13.551	0.279	−0.083
50,401.6448......	50,401.6478	42,427.866	13.564	0.260	−0.083
50,401.6475......	50,401.6505	42,427.939	13.589	0.256	−0.092
50,401.6502......	50,401.6532	42,428.011	13.540	0.273	−0.064
50,401.6528......	50,401.6558	42,428.081	13.558	0.259	−0.098
50,401.6554......	50,401.6584	42,428.150	13.536	0.266	−0.085
50,401.6581......	50,401.6611	42,428.223	13.507	0.242	−0.076
50,401.6608......	50,401.6638	42,428.294	13.474	0.246	−0.058
50,401.6634......	50,401.6664	42,428.363	13.454	0.217	−0.028
50,401.6660......	50,401.6690	42,428.434	13.459	0.198	−0.006
50,401.6686......	50,401.6716	42,428.504	13.459	0.198	−0.030
50,401.6712......	50,401.6742	42,428.574	13.488	0.259	−0.067
50,401.6739......	50,401.6769	42,428.646	13.517	0.256	−0.056
50,401.6766......	50,401.6796	42,428.716	13.542	0.251	−0.073
50,401.6818......	50,401.6848	42,428.856	13.574	0.260	−0.090
50,401.6845......	50,401.6875	42,428.927	13.567	0.271	−0.070
50,401.6871......	50,401.6901	42,428.998	13.564	0.259	−0.049
50,401.6898......	50,401.6928	42,429.069	13.563	0.247	−0.057
50,405.6194......	50,405.6223	42,534.068	13.539	0.233	−0.043
50,405.6217......	50,405.6246	42,534.130	13.540	0.261	−0.061
50,405.6239......	50,405.6268	42,534.188	13.523	0.247	−0.059
50,405.6264......	50,405.6293	42,534.255	13.493	0.248	−0.091
50,405.6286......	50,405.6315	42,534.313	13.450	0.231	−0.022
50,405.6308......	50,405.6337	42,534.372	13.444	0.220	−0.059
50,405.6329......	50,405.6358	42,534.428	13.437	0.197	−0.017
50,405.6351......	50,405.6380	42,534.486	13.449	0.138	−0.028
50,405.6372......	50,405.6401	42,534.543	13.468	0.216	−0.016
50,405.6393......	50,405.6422	42,534.601	13.493	0.208	−0.026
50,405.6416......	50,405.6445	42,534.660	13.499	0.241	−0.005
50,405.6437......	50,405.6466	42,534.717	13.526	0.260	−0.040
50,405.6460......	50,405.6489	42,534.777	13.558	0.252	−0.054
50,405.6480......	50,405.6509	42,534.833	13.563	0.251	−0.076
50,405.6501......	50,405.6530	42,534.889	13.535	0.273	−0.019
50,405.6522......	50,405.6551	42,534.945	13.540	0.277	−0.056
50,405.6543......	50,405.6572	42,535.000	13.561	0.227	−0.061
50,405.6564......	50,405.6593	42,535.056	13.540	0.246	−0.055
50,405.6585......	50,405.6614	42,535.112	13.535	0.227	−0.032
50,405.6606......	50,405.6635	42,535.169	13.512	0.274	−0.087
50,405.6627......	50,405.6656	42,535.224	13.507	0.225	−0.087
50,405.6648......	50,405.6677	42,535.281	13.455	0.244	−0.046
50,405.6669......	50,405.6698	42,535.336	13.445	0.215	−0.052
50,405.6689......	50,405.6718	42,535.391	13.436	0.196	−0.046
50,405.6710......	50,405.6739	42,535.446	13.408	0.237	−0.048
50,405.6730......	50,405.6759	42,535.501	13.433	0.237	−0.041
50,405.6751......	50,405.6780	42,535.556	13.475	0.210	−0.009
50,405.6772......	50,405.6801	42,535.611	13.498	0.236	−0.071
50,405.6792......	50,405.6821	42,535.667	13.505	0.253	−0.038
50,405.6813......	50,405.6842	42,535.722	13.509	0.273	−0.081
50,405.6834......	50,405.6863	42,535.777	13.511	0.267	−0.058
50,405.6856......	50,405.6885	42,535.837	13.541	0.276	−0.075
50,405.6877......	50,405.6906	42,535.894	13.558	0.223	−0.040
50,405.6898......	50,405.6927	42,535.950	13.554	0.223	−0.009
50,405.6920......	50,405.6949	42,536.007	13.555	0.224	−0.061
50,405.6940......	50,405.6969	42,536.062	13.548	0.247	−0.054
50,405.6961......	50,405.6990	42,536.117	13.520	0.247	−0.064
50,405.6981......	50,405.7010	42,536.172	13.525	0.232	−0.097
50,405.7003......	50,405.7032	42,536.228	13.490	0.252	−0.077
50,405.7023......	50,405.7052	42,536.284	13.466	0.222	−0.068

TABLE 2—*Continued*

HJD (2,400,000 +)	HJD + t_{orb}	$n + \varphi$	V	$B-V$	$U-B$
50,405.7044......	50,405.7073	42,536.339	13.430	0.256	−0.079
50,405.7064......	50,405.7093	42,536.393	13.426	0.216	−0.049
50,405.7085......	50,405.7114	42,536.448	13.413	0.231	−0.053
50,405.7106......	50,405.7135	42,536.504	13.426	0.210	−0.005
50,405.7126......	50,405.7155	42,536.559	13.458	0.224	−0.023
50,405.7147......	50,405.7176	42,536.613	13.474	0.246	−0.045
50,405.7167......	50,405.7196	42,536.668	13.516	0.234	−0.061
50,405.7188......	50,405.7217	42,536.723	13.538	0.231	−0.061
50,405.7208......	50,405.7237	42,536.778	13.537	0.258	−0.055
50,405.7229......	50,405.7258	42,536.834	13.540	0.281	−0.061
50,656.8814......	50,656.8834	49,247.882	13.556	0.246	−0.085
50,656.8880......	50,656.8900	49,248.059	13.524	0.252	−0.084
50,656.8903......	50,656.8923	49,248.120	13.496	0.259	−0.085
50,656.8925......	50,656.8945	49,248.180	13.501	0.213	−0.071
50,656.8947......	50,656.8967	49,248.239	13.462	0.227	−0.072
50,656.9003......	50,656.9023	49,248.388	13.520	0.198	−0.052
50,656.9025......	50,656.9045	49,248.447	13.526	0.239	−0.062
50,656.9047......	50,656.9067	49,248.506	13.559	0.247	−0.080
50,656.9100......	50,656.9120	49,248.648	13.576	0.278	−0.080
50,656.9122......	50,656.9142	49,248.706	13.574	0.255	−0.095
50,656.9145......	50,656.9165	49,248.766	13.611	0.237	−0.086
50,656.9196......	50,656.9216	49,248.904	13.661	0.218	−0.073
50,656.9218......	50,656.9238	49,248.962	13.624	0.250	−0.092
50,656.9240......	50,656.9260	49,249.020	13.593	0.267	−0.084
50,656.9291......	50,656.9311	49,249.157	13.550	0.230	−0.077
50,656.9314......	50,656.9334	49,249.218	13.512	0.244	−0.090
50,656.9336......	50,656.9356	49,249.277	13.523	0.254	−0.062
50,656.9358......	50,656.9378	49,249.336	13.557	0.244	−0.068
50,656.9410......	50,656.9430	49,249.476	13.536	0.330	0.004
50,658.7885......	50,658.7905	49,298.842	13.602	0.243	−0.028
50,658.7907......	50,658.7927	49,298.901	13.616	0.236	−0.035
50,658.7930......	50,658.7950	49,298.961	13.613	0.253	−0.082
50,658.7982......	50,658.8002	49,299.101	13.668	0.224	−0.078
50,658.8005......	50,658.8025	49,299.161	13.495	0.239	−0.068
50,658.8057......	50,658.8077	49,299.301	13.520	0.215	−0.046
50,658.8079......	50,658.8099	49,299.361	13.545	0.201	−0.011
50,658.8150......	50,658.8170	49,299.550	13.532	0.235	−0.045
50,658.8174......	50,658.8194	49,299.613	13.557	0.229	−0.029
50,658.8226......	50,658.8246	49,299.752	13.580	0.238	−0.062
50,658.8248......	50,658.8268	49,299.811	13.596	0.221	−0.042
50,658.8300......	50,658.8320	49,299.950	13.565	0.241	−0.028
50,658.8322......	50,658.8342	49,300.009	13.561	0.214	−0.023
50,658.8346......	50,658.8366	49,300.074	13.540	0.226	−0.049
50,658.8396......	50,658.8416	49,300.207	13.484	0.216	−0.036
50,658.8418......	50,658.8438	49,300.265	13.467	0.202	−0.034
50,658.8442......	50,658.8462	49,300.330	13.467	0.199	−0.017
50,658.8465......	50,658.8485	49,300.390	13.471	0.221	−0.037
50,658.8488......	50,658.8508	49,300.452	13.494	0.225	−0.045
50,658.8539......	50,658.8559	49,300.588	13.554	0.230	−0.051
50,658.8562......	50,658.8582	49,300.649	13.556	0.233	−0.054
50,658.8615......	50,658.8635	49,300.791	13.594	0.223	−0.032
50,658.8637......	50,658.8657	49,300.850	13.598	0.218	−0.030
50,658.8659......	50,658.8679	49,300.911	13.580	0.240	−0.084
50,658.8688......	50,658.8708	49,300.987	13.562	0.232	−0.068
50,658.8739......	50,658.8759	49,301.125	13.515	0.232	−0.072
50,658.8762......	50,658.8782	49,301.185	13.487	0.207	−0.031
50,658.8785......	50,658.8805	49,301.246	13.465	0.223	−0.037
50,658.8807......	50,658.8827	49,301.305	13.453	0.225	−0.040
50,658.8829......	50,658.8849	49,301.364	13.477	0.211	−0.039
50,658.8880......	50,658.8900	49,301.501	13.517	0.209	−0.022
50,658.8903......	50,658.8923	49,301.561	13.535	0.213	−0.011
50,658.8926......	50,658.8946	49,301.624	13.560	0.227	−0.051
50,658.8977......	50,658.8997	49,301.759	13.591	0.226	−0.058
50,658.9000......	50,658.9020	49,301.820	13.647	0.218	−0.035
50,658.9022......	50,658.9042	49,301.880	13.590	0.228	−0.065
50,658.9073......	50,658.9093	49,302.016	13.542	0.250	−0.043
50,658.9096......	50,658.9116	49,302.078	13.524	0.244	−0.064
50,658.9148......	50,658.9168	49,302.216	13.460	0.233	−0.057
50,658.9169......	50,658.9189	49,302.273	13.451	0.212	−0.050
50,658.9192......	50,658.9212	49,302.334	13.462	0.205	−0.033
50,658.9215......	50,658.9235	49,302.395	13.471	0.204	−0.029
50,658.9265......	50,658.9285	49,302.528	13.516	0.207	−0.035
50,658.9287......	50,658.9307	49,302.587	13.556	0.237	−0.090

TABLE 2—*Continued*

HJD (2,400,000 +)	HJD + t_{orb}	$n + \varphi$	V	$B-V$	$U-B$
50,720.7147......	50,720.7180	50,953.573	13.497	0.244	−0.038
50,720.7169......	50,720.7202	50,953.631	13.523	0.245	−0.046
50,720.7193......	50,720.7226	50,953.697	13.539	0.248	−0.053
50,720.7245......	50,720.7278	50,953.835	13.560	0.264	−0.077
50,720.7267......	50,720.7300	50,953.894	13.559	0.256	−0.045
50,720.7290......	50,720.7323	50,953.957	13.564	0.249	−0.045
50,720.7340......	50,720.7373	50,954.088	13.542	0.259	−0.058
50,720.7362......	50,720.7395	50,954.149	13.525	0.249	−0.072
50,720.7385......	50,720.7418	50,954.209	13.495	0.241	−0.053
50,720.7433......	50,720.7466	50,954.339	13.435	0.238	−0.040
50,720.7456......	50,720.7489	50,954.399	13.454	0.225	−0.051
50,720.7479......	50,720.7512	50,954.460	13.451	0.250	−0.053
50,720.7504......	50,720.7537	50,954.528	13.479	0.251	−0.051
50,720.7558......	50,720.7591	50,954.671	13.535	0.254	−0.067
50,720.7581......	50,720.7614	50,954.733	13.537	0.268	−0.065
50,720.7604......	50,720.7637	50,954.795	13.547	0.278	−0.074
50,720.7630......	50,720.7663	50,954.864	13.553	0.270	−0.058
50,720.7680......	50,720.7713	50,954.999	13.533	0.272	−0.055
50,720.7706......	50,720.7739	50,955.067	13.541	0.264	−0.066
50,720.7755......	50,720.7788	50,955.199	13.511	0.236	−0.074
50,720.7778......	50,720.7811	50,955.260	13.454	0.242	−0.061
50,720.7801......	50,720.7834	50,955.321	13.431	0.247	−0.051
50,720.7824......	50,720.7857	50,955.384	13.440	0.223	−0.056
50,720.7847......	50,720.7880	50,955.444	13.447	0.232	−0.049
50,720.7871......	50,720.7904	50,955.507	13.469	0.241	−0.039

observations made in 1996 August and November. In addition, the phase relation between the two data sets was not known a priori. It seemed best to derive pulsation elements (period, initial epoch, velocity amplitude) from all the velocity data collected during the much longer time interval 1992 through 1997, but a problem evident in Figure 1 (*top*) was immediately encountered: the mean velocity varies from year to year, as listed in Table 3. To remove the annual velocity shifts, we first constructed a velocity versus phase diagram for the most numerous 1996 observations by use of a provisional period, 0.0374 days. We fitted a sinelike velocity curve to the 1996 data combined in this manner and adopted it as a template pulsation curve. The mean velocity and zero point of phase (taken to be a time of velocity maximum) were then adjusted to fit this curve to the radial velocities obtained in each of the other years. Finally, annual mean velocity corrections RV(1996) minus RV(year) were added to all velocities to bring them into coincidence with the 1996 velocity curve, and the period was tweaked to minimize systematic annual phase residuals. The result is shown in Figure 1 (*bottom*), where phases for the corrected radial velocities are calculated with the period $P = 0.03742449$ days from

$$n + \varphi = (\mathrm{HJD}_c - 2{,}448{,}813.8065)/0.03742449 \ , \quad (1)$$

TABLE 3

ORBITAL RADIAL VELOCITIES OF CS 22966−043

Year	⟨HJD⟩ (2,400,000+)	⟨RV⟩ (km s^{-1})
1992...........	48,818.79	−267.0
1993...........	49,201.27	−274.0
1994...........	49,585.09	−274.0
1995...........	49,939.78	−270.0
1996...........	50,291.33	−261.7
1997 Jul	50,646.81	−258.5
1997 Sep......	50,704.71	−262.0

where n is the cycle count, φ is the cycle fraction, and HJD_c is the Heliocentric Julian Date corrected for orbital light-travel time as described in § 4. Note that more than 50,000 pulsation cycles occurred between the first and last spectroscopic observations. We estimate the error of the period from $\epsilon(P) \approx \pm P^2 \Delta\phi/(t_f - t_i)$, in which $\Delta\phi$ is the minimum detectable systematic phase shift of yearly observations from the mean velocity curve at final and initial epochs t_f and t_i, respectively. Conservatively, we restrict our attention to the epochs 1994 (JD 2,449,584) and 1997 (JD 2,450,704) and use $\Delta\phi = 0.05$ to calculate $\epsilon(P) = \pm 0.00000007$. Observations in 1992 and 1993 near phase $\varphi = 0.5$ fall more or less midway between the standard pulsation curve and the mean velocity because the integration times of these particular observations, made before the short pulsation cycle was recognized, were long, amounting to approximately one-half and one-third of the pulsation period, respectively.

All the radial velocities derived from spectra obtained in 1997 June and 1997 July are afflicted by unrecoverable optical vignetting errors of electromechanical origin in the spectrograph that were not recognized during the observations (a failing potentiometer produced improper, nonrepeating, centering of the apertures of the spectrograph filter wheel). The filter wheel is rotated before each star/ThAr observation to remove/insert neutral density filters. From 23 measurements of 14 BMP standard stars, we found that the errors produced by this vignetting ranged from 0 to +4 km s^{-1}, the average being +1.7 km s^{-1}. Accordingly, we corrected all the 1997 July velocities by −1.7 km s^{-1}. These observations (coded as J's in Fig. 1) have systematically larger velocity residuals than the remainder of the data, and they were given lowest weight in the period-fitting process.

3.2. *Photometric Variations*

The stability of the photometric variations of CS 22966−043 can be judged from the separate plots of the

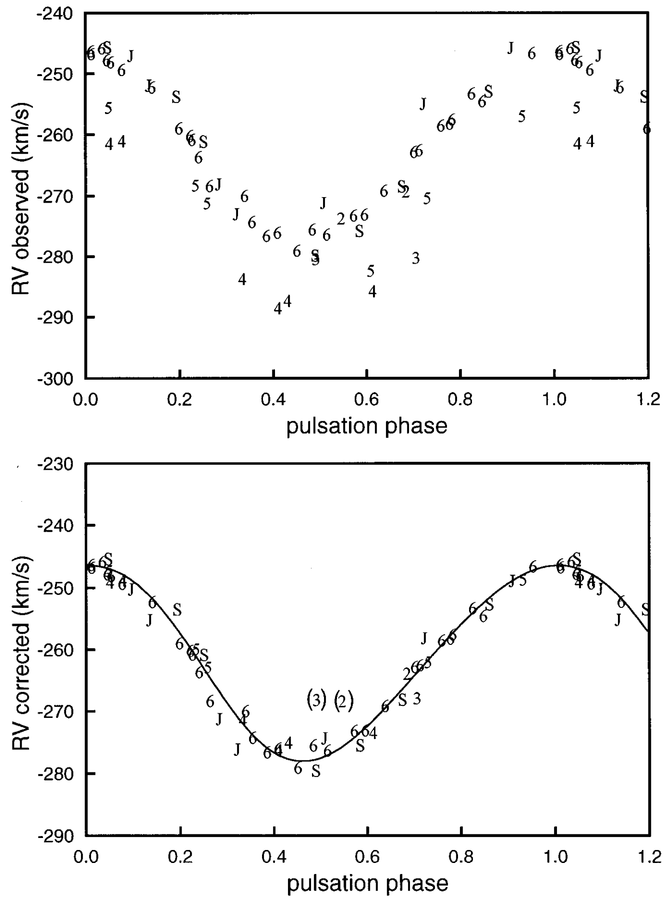

FIG. 1.—*Top:* Observed radial velocities of CS 22966−043 plotted vs. phases calculated by use of eq. (1). Numerical symbols denote the year in which observations were made. The letters J and S denote observations made in 1997 July and September, respectively. The vertical displacements of observations made in different years are clearly evident. *Bottom:* Radial velocities corrected for the orbital radial velocities of the primary star given in Table 5. The symbols "(2)" and "(3)" denote observations with long integration times, as discussed in the text.

V-magnitude variations at four epochs in 1996 and 1997 shown in the four panels of Figure 2. Pulsation cycles are coded by night with the letters A through L in Figure 2 and Table 4, which gives times of light maximum for each observed cycle. It is evident that the pulsation of the star is stable. The variations in apparent maxima and minima from night to night, month to month, and year to year are no larger than a few hundredths of a magnitude at most, amounts that reflect zero-point uncertainties of the magnitude scales derived for the various nights. The night of July 27 (code J) is the one glaring exception, and A. U. L.'s observing log duly notes that this night was of inferior quality. Accordingly, we believe that it is justifiable to combine all the velocity and photometric data into single phase diagrams. This has been done for the photometry in Figure 3, which shows the V, $B-V$, and $U-B$ variations of CS 22966−043. The $B-V$ color is bluest at maximum light, while $U-B$ varies in antiphase. The effect of the two color variations is to move the star more or less parallel to the main sequence in the ($U-B$, $B-V$)-plane as expected if temperature varies periodically during the pulsation cycle. In these respects CS 22966−043 is an ordinary pulsating star.

TABLE 4

HELIOCENTRIC JULIAN DATES OF VISUAL LIGHT MAXIMUM

Night	HJD(V_{max})	Q[a]	Night	HJD(V_{max})	Q[a]
A	2,450,312.8914		G	2,450,397.6240	
B	2,450,314.8753		G	2,450,397.6984	
C	2,450,315.8483		H	2,450,401.6286	
C	2,450,315.8861		H	2,450,401.6652	
D	2,450,316.7460		I	2,450,405.6323	
D	2,450,316.7839		I	2,450,405.6700	
D	2,450,316.8210		I	2,450,405.7079	
E	2,450,318.7676		J	2,450,656.8958	:
E	2,450,318.8054		J	2,450,656.9341	:
E	2,450,318.8433		K	2,450,658.8438	
E	2,450,318.8799		K	2,450,658.8811	
E	2,450,318.9163	:	K	2,450,658.9180	
F	2,450,396.5757		L	2,450,720.7441	
F	2,450,396.6129		L	2,450,720.7818	

[a] Colon indicates lower quality data.

4. THE BINARY ORBIT AND LIGHT-TRAVEL TIME CORRECTIONS

We derived a binary orbit with the elements given in Table 5 from the mean velocities in Table 3. The radial velocity curve calculated from these elements is shown in Figure 4. The relatively small amplitude of the orbital motion was masked by the dominant pulsation amplitude and thus escaped prior detection. The 1992–1996 data admit of two additional long periods, ∼200 days and some long period ≥2300 days. The change in velocity between 1997 July and 1997 September seems to rule out both these alternatives, but we remain cautious because of the flawed 1997 July data. As noted at the end of this section, orbital light-time corrections seem to rule out the 2300 day period. Observations in 1998 and thereafter will be required to establish the orbital period beyond doubt.

We integrated the radial velocity curve to obtain the time variation of distance to the star due to orbital motion. Division of this oscillating distance, $\Delta R(\varphi)$, by the velocity of light then produces the variation of light-travel time across the apparent orbit of the binary as a function of orbital phase, shown in Figure 5. The light-travel time varies by almost 0.004 days, i.e., 10% of the pulsation period of the star, during an orbital revolution, so it is desirable to add this quantity to the HJD, if data from different orbital epochs are to be combined with minimal phase dispersion by use of the uniform ephemeris in equation (1): hence the use of corrected Heliocentric Julian Days HJD_c in equation (1).

Orbital light-travel time corrections calculated for the 2300 day period are comparable to the pulsation period itself, and their use hopelessly jumbles the velocity and photometric data. Therefore, we believe that $P \approx 200$ days is the only possible alternative to our adopted orbital period.

TABLE 5

SPECTROSCOPIC BINARY ORBITAL ELEMENTS

Parameter	Value
HJD(RV_{max})	48,385
V_γ (km s^{-1})	−266.4
K_1 (km s^{-1})	8.1
e	0.10
ω (deg)	260
P (days)	431

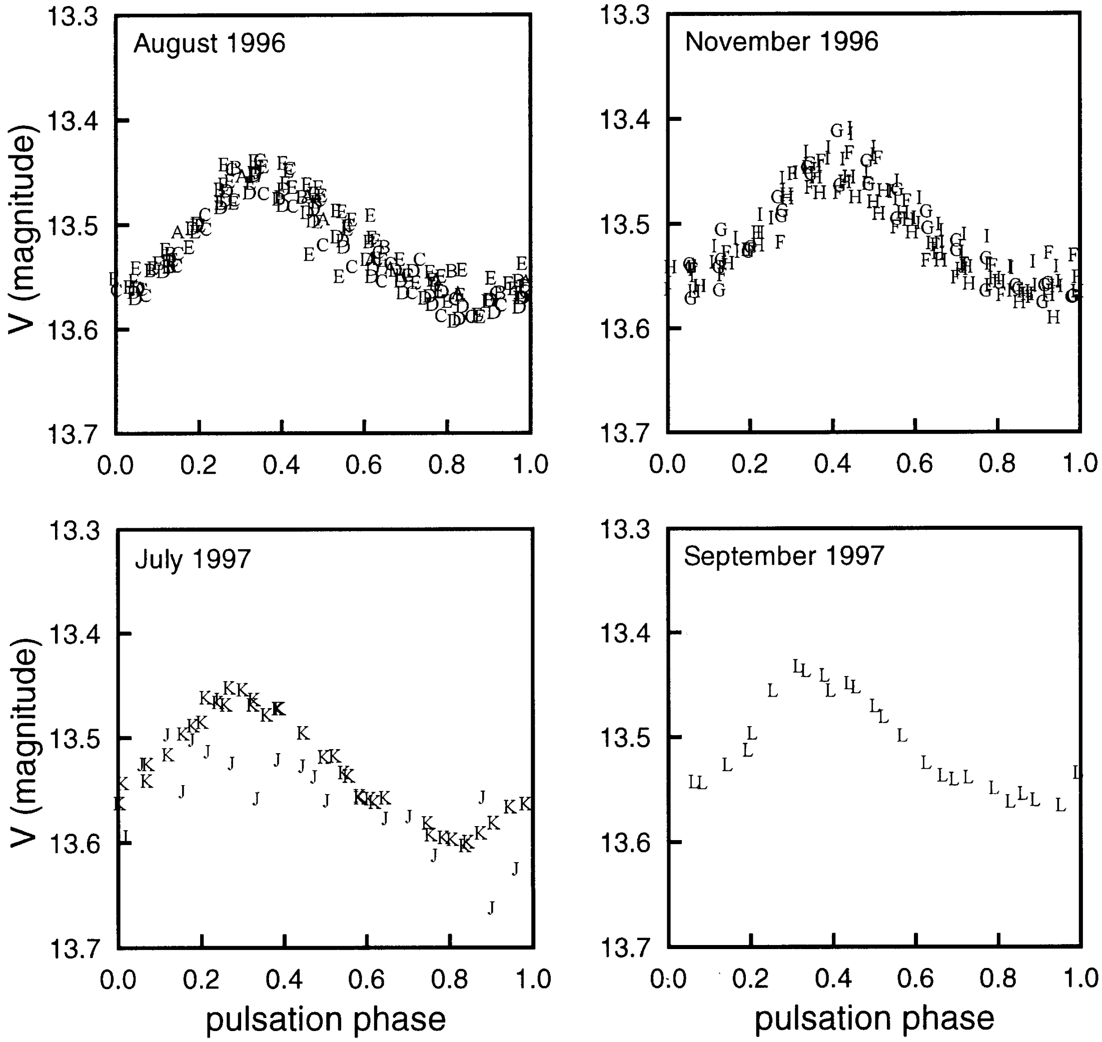

FIG. 2.—Visual magnitudes of CS 22966−043 plotted vs. phases calculated by use of eq. (1) for observations made at four different epochs in 1996 and 1997. The letters denote observations made on the various nights listed in Table 4. With the exception of the inferior data of night J, all of the observations appear to define a pulsation light curve with constant amplitude.

5. COMPARISON OF OBSERVED VISUAL LIGHT VARIATION WITH THAT CALCULATED FROM THE RADIAL VELOCITY AND $B-V$ COLOR VARIATIONS

We calculate the light variation of the star as the product of surface brightness and area, proportional to $R^2T_e^4$, in which effective temperature T_e is estimated from an appropriate $T_e = f(B-V)$ relation and stellar radius is calculated from

$$R(\phi) = \langle R \rangle + \Delta R(\phi) , \quad (2)$$

where $\langle R \rangle$ is a plausible adopted mean radius, here assumed to be 1.5 $R_\odot$, and $\Delta R(\phi)$ is obtained from integration of the pulsation velocity, here taken to be -1.3 times the radial velocity (Parsons 1972). The displacement curve due to pulsation is shown in Figure 6 (*top*). The $B-V$ color index variation shown in Figure 6 (*middle*) is a hand-drawn curve through mean points calculated from the data shown in Figure 3 (*middle*) at intervals of 0.05P. In view of the negligible reddening deduced by Burstein & Heiles (1982) in the direction toward CS 22966−043 ($l = 25°$, $b = -76°$), we assume that the observed colors are intrinsic colors. We know of no fundamental data on effective temperatures of metal-poor A-type main-sequence stars, so we estimated as follows: We began with the main-sequence $T_e = f(B-V)$ relation for solar-type stars of Böhm-Vitense (1981). To these colors we added the differences in $B-V$ colors calculated by Kurucz (unpublished) for models with [Fe/H] = -2 and 0 at log $g = 4$. These theoretical colors differ only slightly from the earlier calculations of Buser & Kurucz (1978). By this procedure for deblanketing the Böhm-Vitense colors, we hope to minimize the inevitable zero-point errors in the Kurucz color scales. The procedure gives $T_e = 7260$ K at $B-V = 0.25$ with slope $dT_e/d(B-V) = -6250$ K mag^{-1}. As a check, we constructed a relation from the turnoff colors and effective temperatures of the Revised Yale Isochrones (Green, Demarque, & King 1987) for $Z = 0.0001$ and obtained $T_e = 7380$ K at $B-V = 0.25$ with slope $dT_e/d(B-V) = -7790$ K mag^{-1}. We averaged the coefficients of the two estimates to obtain $T_e = 7320 - 7000[(B-V) - 0.25]$, or

$$T_e = 9070 - 7000(B-V) , \quad (3)$$

which produces effective temperatures that agree with both calibrations to within 100 K over the small color range of this star. Calculating $R(\varphi)$ from equation (2) and effective temperatures from equation (3) and the color curve in

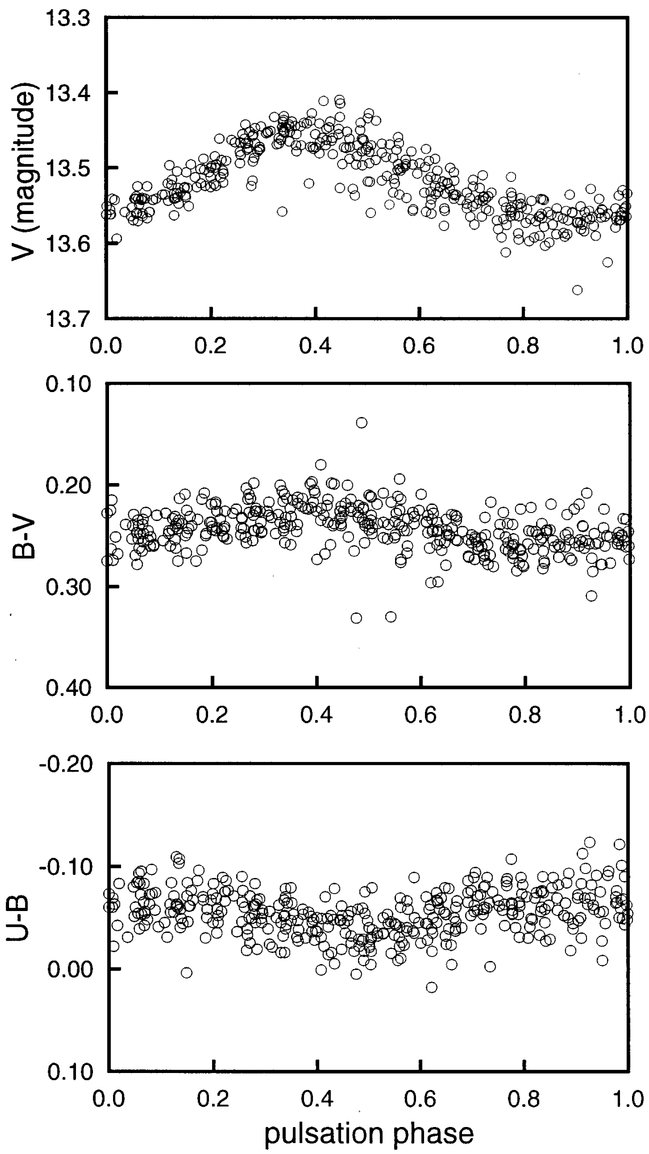

FIG. 3.—V, $B-V$, and $U-B$ variations of CS 22966−043 defined by all of the data in Table 2 and Fig. 2.

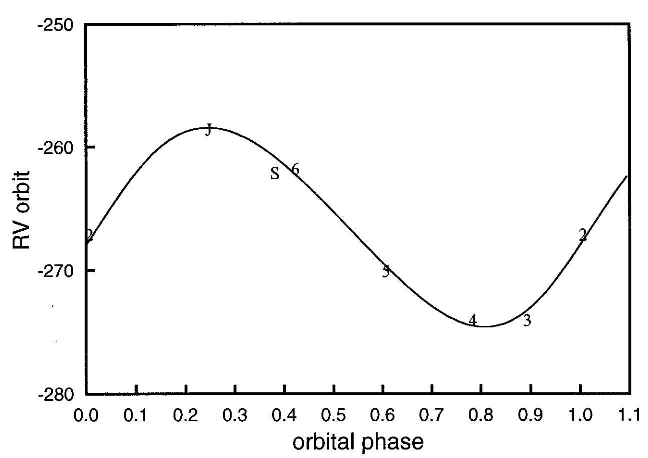

FIG. 4.—Orbital radial velocities of CS 22966−043 in Table 3 plotted vs. phase calculated by use of the elements in Table 5. The curve is also calculated by use of the orbital elements in Table 5. The symbol code is the same as that in Fig. 1.

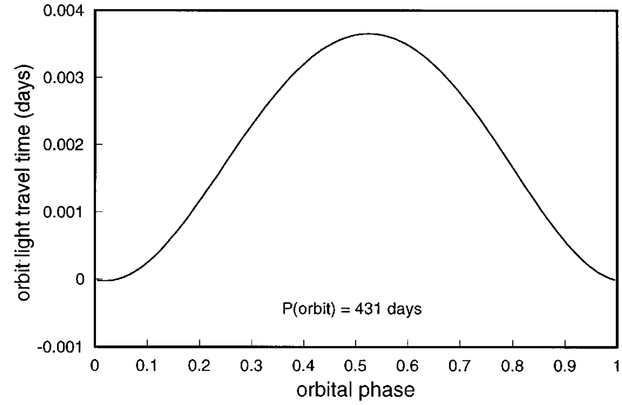

FIG. 5.—Orbital light-travel time for CS 22966−043 plotted vs. orbital phase. The range of the light-travel time is about 1/10 of the pulsation period.

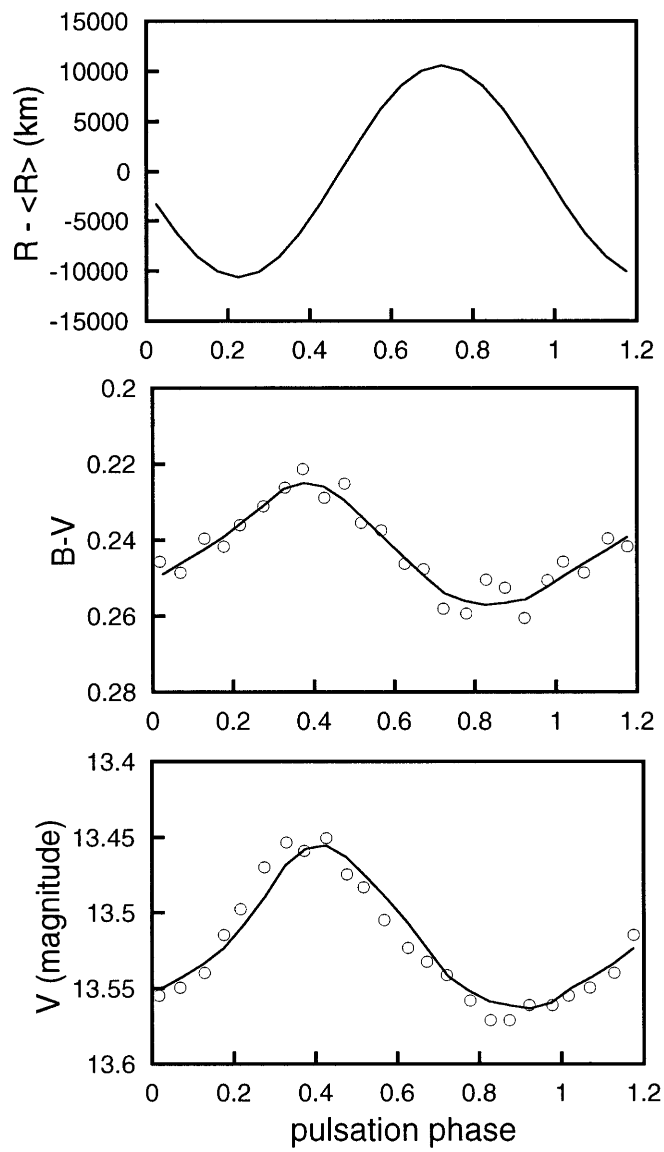

FIG. 6.—*Top:* Pulsation displacement curve obtained by integrating the pulsation velocity curve as discussed in the text. *Middle:* A freehand curve has been drawn through mean points of the $B-V$ data in Table 2 (*circles*). *Bottom:* Light variation calculated by use of eq. (4) is plotted together with mean points of the V magnitude data in Table 2 (*circles*).

Figure 6 (*middle*), we obtain the calculated curve in Figure 6 (*bottom*) from

$$V(\varphi) = 13.52 - 2.5 \log \{[R(\varphi)/\langle R \rangle]^2 [T_e(\varphi)/\langle T_e \rangle]^4\} . \quad (4)$$

The symbols in Figure 6 (*bottom*) again denote mean points calculated at intervals of $0.05P$. The bolometric correction to the V magnitude is small and remains virtually constant during small temperature variations near $T_e = 7500$ K, so it is simply absorbed into the fitting constant in equation (4). The calculated curve agrees with the observations to within ± 0.02 mag at all phases, so we are satisfied that the observed light variation of CS 22966−043 is compatible with the observed color and radial velocity variations.

6. DISCUSSION

First of all we note the striking resemblance of CS 22966−043 to the SX Phoenicis stars in NGC 5063. Five of 11 blue stragglers (BSs) investigated for variability by Nemec et al. (1995) are pulsating variables with periods in the narrow range 0.03416–0.03925 days. CS 22966−043 lies near the middle of this range. Four of the cluster variables, pulsating in the fundamental mode, lie in the narrow color range $0.20 < (B-V)_0 < 0.27$, which brackets the mean color $\langle B-V \rangle = 0.24$ of CS 22966−043. Finally, the metal abundance of CS 22966−043 ([Fe/H] ≈ -2.4), estimated from the location of the star in Figure 1 of Preston (1995), is indistinguishable from that of NGC 5053 ([Fe/H] = −2.41). Considering that analogs of the globular cluster variables ought to be present in the field, we consider it likely that CS 22966−043 is indeed a field example of the NGC 5053 SX Phoenicis stars, rather than an accreted intermediate-age main-sequence star. As such, it has the shortest period among known field SX Phoenicis stars as defined in Table 1 of Nemec & Mateo (1990) or in Table 3 of Mateo (1993). The comparison with SX Phoenicis stars in NGC 4372 (Kaluzny & Krzeminski 1993) is not so favorable. Although the cluster abundance is similar, [Fe/H] = −2.35, according to Geisler, Minniti, & Claria (1992), the pulsation period of CS 22966−043 lies outside the range in NGC 4372, 0.041 days $< P <$ 0.067 days. The period distributions of SX Phoenicis stars in these two clusters do not even overlap; clearly, some additional parameter besides abundance affects the pulsation periods of SX Phoenicis stars of similar color and luminosity in these two clusters. A thorough exploration of the period distributions of SX Phoenicis stars among the BSs in more globular clusters with a range of central concentrations and abundances may help to explicate this enigma.

Identification of CS 22966−043 as a pulsating BS places a modest constraint on the BS fraction of the BMP population. It is certain that CS 22966−043 is the only SX Phoenicis star in the BMP sample of 62 stars investigated for velocity variability. In three globular clusters investigated with some care, from 13% to 31% of BSs are SX Phoenicis stars: six of 47 in NGC 5466 (Mateo et al. 1990), five of 16 in NGC 5053 (Nemec et al. 1995), and eight of 40 in NGC 4372 (Kaluzny & Krzeminski 1993). The smaller proportion of SX Phoenicis stars in the BMP sample, one of 60, suggests to us that globular cluster–like BSs comprise but a small fraction of the BMP sample.

Finally, CS 22966−043 provides food for thought about the process by which this particular pulsating blue straggler was formed. It is generally believed that BSs owe their origin to binary mass transfer interactions. In the halo field stellar collisions do not happen, and the only other binary interaction mechanisms are merger and mass transfer during post–main-sequence evolution of the primordial primary. For stars with masses of $\sim 1\ M_\odot$ the former process is restricted to binaries with initial periods less than ~ 5 days (Vilhu 1982), while the latter process can occur for a much larger range of initial separations. Mateo et al. (1990) used estimates of the merger timescale and BS lifetimes to argue that merger is the primary mechanism in NGC 5466. We suggest that CS 22966−043 is more likely to have been formed by mass transfer than merger, in which case the unseen secondary is the degenerate relic of its former self. The merger process would require that this particular SX Phoenicis star, a rare stellar species to begin with, began its life as the primary of a close binary in a triple system, itself a rare configuration. We prefer the use of Occam's razor in this instance.

We acknowledge with thanks the aid of the staffs of CTIO and Las Campanas Observatory, respectively. A. U. L.'s research is supported by NSF grant AST 95-28177.

REFERENCES

Böhm-Vitense, E. 1981, ARA&A, 19, 295
Burstein, D., & Heiles, C. 1982, AJ, 87, 1165
Buser, R., & Kurucz, R. L. 1978, A&A, 70, 555
Geisler, D., Minniti, D., & Claria, J. J. 1992, AJ, 104, 627
Green, E. M., Demarque, P., & King, C. R. 1987, The Revised Yale Isochrones and Luminosity Functions (New Haven: Yale Univ. Obs.)
Kaluzny, J., & Krzeminski, W. 1993, MNRAS, 264, 785
Landolt, A. U. 1992, AJ, 104, 340
Mateo, M. 1993, in ASP Conf. Ser. 53, Blue Stragglers, ed. R. A. Saffer (San Francisco: ASP), 74
Mateo, M., Harris, H. C., Nemec, J., & Olszewski, E. W. 1990, AJ, 100, 469
Nemec, J., & Mateo, M. 1990, in ASP Conf. Ser. 11, Confrontation between Stellar Pulsation and Evolution, ed. C. Cacciari & G. Clementini (San Francisco: ASP), 64
Nemec, J. M., Mateo, M., Burke, M., & Olszewski, E. W. 1995, AJ, 110, 1186
Parsons, S. B. 1972, ApJ, 174, 57
Preston, G. W. 1994, AJ, 108, 2267
———. 1995, in ASP Conf. Ser. 92, Formation of the Galactic Halo—Inside and Out, ed. H. Morrison & A. Sarajedini (San Francisco: ASP), 49
Preston, G. W., Beers, T. C., & Shectman, S. A. 1994, AJ, 108, 538
Shectman, S. A. 1984, Proc. SPIE, 445, 128
Vilhu, O. 1982, A&A, 109, 17